Maximum Spectral Flatness Control of a Manipulandum for Human Motor System Identification

Yingxin Qiu[1], Mengnan Wu[2], Lena H. Ting[3], and Jun Ueda[1]

***Abstract*—System identification of a dynamic environment using a robotic device utilizes physical perturbations in the form of displacement or force. To obtain an accurate system model, physical perturbations must be informative, which can be characterized by their spectral properties. The process of generating physical perturbations by using a robotic device often leads to spectral property degradation in the high-frequency region due to the dynamics of robot motion control and discrete-time signal processing. Spectral flatness is a metric applicable to quantifying the fidelity of the robotic system and quality of physical perturbations on an external object. This paper introduces a new metric named Band-limited Spectral Flatness Gain (BLSFG) to evaluate the physical perturbation quality relative to the input reference over a frequency band of interest. Motion control of a manipulandum that generates pseudorandom position perturbations for human sensorimotor system identification is considered as a representative example. The closed-loop system dynamics of the position control is characterized and optimized based on the BLSFG. Results suggest that a certain underdamped closed-loop property is advantageous to improve the spectral flatness of a degraded continuous-time pseudorandom reference. A high BLSFG is achieved when the resonance frequency of the closed-loop system is close to the update frequency of the pseudorandom sequence.**

***Index Terms*—Motion Control, Physical Human-Robot Interaction, Spectral Flatness, System Identification**

I. Introduction

SYSTEM identification of a dynamic environment using an active device is a widely-used methodology in engineering and science including applications in factory automation [1], [2] and biomedicine [3], [4]. In human-scale applications, physical perturbations are generated by a robotic device such as a manipulator, a mobile platform, or a haptic device, and applied to the environment of interest in the form of force or displacement [5], [6]. While desired properties of physical perturbations vary depending on the characteristics of the environment being identified, perturbations should satisfy the persistent excitation (PE) condition characterized by their spectral properties - that is, perturbations should contain sufficient frequency components that excite a sufficient number of modes in the target systems [7]. A robotic device takes a perturbation reference command and realizes the physical perturbation with a motion controller. Since the robotic device is itself a dynamic system usually controlled by a digital computer, the process of generating physical perturbations by using a robotic device often leads to spectral property degradation in the high-frequency region due to the dynamics of robot motion control and discrete-time signal processing. This filtering effect due to the robot dynamics has often been overlooked. To maintain the desired spectral properties of physical perturbations, high-fidelity motion control should be implemented.

In this paper, generating position perturbations with a manipulandum for human sensorimotor system identification is considered as a representative example. For human system identification, recent work has shown that the human nervous system is very sensitive to high-frequency signals, and thus perturbations should contain high-frequency components to probe the higher frequency responses of biological systems that are not simply due to inertia [8]–[10]. Note that achieving the PE condition by a frequency sweep is inappropriate due to the predictability of the perturbation patterns as well as its time-consuming nature. A pseudorandom ternary sequence (PRTS), which is a three-level deterministic sequence with white-noise-like properties, is a reasonable alternative and has been used in human experiments as a physical perturbation reference for its randomness and flat spectrum properties [6], [11]–[13]. In previous applications of PRTS, physical perturbations applied to human subjects were generated by a certain combination of PRTS integration, interpolation, discrete-to-continuous-time conversion, realized in an experimental motion platform with a limited control bandwidth. Such implementation should have altered the ideal properties of the original random sequences; however, the spectral property degradation issues were rarely addressed. A measure of perturbation quality is needed to quantify such effects and to guide the motion controller design for improved perturbation quality.

Spectral flatness is a metric that can be used to quantify the fidelity of the robotic system and quality of physical

Manuscript received: October 15, 2020; Revised January 21, 2021; Accepted February 12 2021. This paper was recommended for publication by Editor Jee-Hwan Ryu upon evaluation of Reviewers' comments. This work was supported by National Science Foundation under Grant Nos. CMMI-M3X 1761679 and 1762211.

[1]Yingxin Qiu and Jun Ueda are with the George W. Woodruff School of Mechanical Engineering, Georgia Institute of Technology, Atlanta, GA 30332-0405, USA. (e-mail: yqiu47@gatech.edu; jun.ueda@me.gatech.edu)

[2]Mengnan Wu is with the W. H. Coulter Department of Biomedical Engineering, Emory University and Georgia Institute of Technology, Atlanta, GA 30332-4250, USA. (e-mail: mengnan.wu@emory.edu)

[3]Lena H. Ting is with the W. H. Coulter Department of Biomedical Engineering, Emory University and Georgia Institute of Technology, and Department of Rehabilitation Medicine, Division of Physical Therapy, Emory University, Atlanta, GA 30332-4250, USA. (e-mail: lting@emory.edu)

Digital Object Identifier (DOI): see top of this page.

perturbations on an external object. This paper introduces a new metric named Band-limited Spectral Flatness Gain (BLSFG) to evaluate the physical perturbation quality relative to the input reference over a frequency band of interest. The closed-loop system dynamics of the position control is characterized and optimized based on the BLSFG.

II. Problem Statement

Physical perturbations must have sufficient randomness and persistence of excitation for effective human motor system identification. The randomness of a signal can be analyzed by its autocorrelation function (ACF), which reflects the temporal self correlation of the signal [14]. A perfectly random signal exhibits no correlation with time-delayed versions of itself. Hence, perfect randomness is represented by an ACF of a (scaled) delta function, with a single peak at zero time delay and zeros otherwise. For example, a single impulse has an ACF of a delta function and therefore is unpredictable. The PE condition can be met by using a perturbation with a flat spectrum. A perfectly flat spectrum not only satisfies the PE condition, but also ensures an equal power distribution over a range of frequencies. The flatness of a spectrum can be quantified by the spectral flatness measure (SFM) [15]. A perfectly flat spectrum has an SFM of 1 and frequency components of equal magnitude. A combination of ACF and SFM can quantify the quality of physical perturbations for human sensorimotor system identification. Note that a perfectly random signal has a delta function as its ACF, and a delta function has a flat spectrum. Therefore, perfect randomness coincides with a perfect spectral flatness. In the following, the analysis focuses on the spectral flatness of random perturbations.

PRTS is a suitable perturbation signal for human experiments due to its high autocorrelation and spectral flatness as shown in Fig. 1(a) (left). Given a PRTS, the process in Fig. 1(a) will generate physical perturbations from a discrete-time sequence. In the first step, a zero-order hold (ZOH) (or other data-holding operation) converts the discrete sequence into a continuous-time signal (Fig. 1(a) (center)). The signal spectrum modulated by the ZOH exhibits highly attenuated components beyond the PRTS update frequency, resulting in a severe degradation of performance. In the second step, the continuous-time reference is physically realized by a manipulandum (Fig. 1(a) (right)). The modulation of the spectral flatness due to the manipulandum dynamics depends on the implemented motion control. As will be addressed in a later section, a properly designed motion controller can improve the SFM with respect to that of the ZOH PRTS over a certain range of frequency. The objective of this paper is to establish a motion control design methodology for improved dynamic system identification based on the SFM.

Section III provides the definition of the SFM. The concept of BLSFG is introduced to quantify the fidelity of motion control over a specified frequency band. In Section IV, three cases of BLSFG are presented. A phase-lead compensator of a position-controlled manipulandum is tuned and evaluated.

III. Spectral flatness measure

The spectral flatness measure (SFM) quantifies the flatness of a signal spectrum. It measures how flat a signal spectrum is as the ratio of its geometric mean to its arithmetic mean. Given a finite energy time sequence $x(n)$, the spectral flatness measure is defined as [15]

$$\gamma_x^2 = \frac{\exp[\frac{1}{2\pi}\int_{-\pi}^{\pi}\log S_{xx}(e^{j\theta})d\theta]}{\frac{1}{2\pi}\int_{-\pi}^{\pi}S_{xx}(e^{j\theta})d\theta} = \frac{\eta_x^2}{\sigma_x^2} \tag{1}$$

where $\gamma_x^2 \in (0,1]$ is the SFM, $S_{xx}(e^{j\theta})$ is the power spectrum of $x(n)$, and η_x^2 and σ_x^2 are the geometric mean and arithmetic mean of the spectrum, respectively. The arithmetic mean is equivalent to the autocorrelation function at zero delay, $R_{xx}(0)$. The discrete expression of the SFM is given by

$$\gamma_x^2 = \frac{\exp[\frac{1}{N}\sum_{n=0}^{N-1}\log S_{xx}(n)]}{\frac{1}{N}\sum_{n=0}^{N-1}S_{xx}(n)}. \tag{2}$$

The spectral flatness measure has a maximum value of 1 and is lower bounded by 0. The closeness of an autocorrelation function to a delta function (not uniquely defined) is not necessarily the flatness of the spectrum; however, perfect randomness coincides with perfect spectral flatness. Since the control objective is to achieve both, it is not unreasonable to lump the two performance measures and use SFM to quantify the performance of a perturbation.

A. Spectral flatness gain

A pseudorandom sequence, after a data-holding operation, has a degraded spectral flatness. The spectral flatness may be further degraded by the closed-loop system dynamics. To isolate the spectral flatness modulation due to the closed-loop system dynamics, an output-to-input spectral flatness gain is defined. Given a discrete-time linear time-invariant system

$$Y(z) = G(z)X(z) \tag{3}$$

with the input $X(z)$, transfer function $G(z)$, and output $Y(z)$, the output SFM γ_y^2 is a function of the input SFM γ_x^2 and transfer function spectral properties. In [16], the relationship between γ_y^2 and γ_x^2 was established with an all-zero filter $G(z)$ for linear prediction of audio signals. In the following, the spectral flatness gain is defined for a general transfer function $G(z)$.

From the definition of SFM, the output spectral flatness is

$$\begin{aligned}\gamma_y^2 &= \frac{\exp\left[\frac{1}{2\pi}\int_{-\pi}^{\pi}\log S_{yy}(e^{j\theta})d\theta\right]}{\frac{1}{2\pi}\int_{-\pi}^{\pi}\log S_{yy}(e^{j\theta})d\theta}. \\ &= \frac{\exp\left[\frac{1}{2\pi}\int_{-\pi}^{\pi}\log\left[|G(e^{j\theta})|^2|X(e^{j\theta})|^2\right]d\theta\right]}{R_{yy}(0)} \\ &= \frac{\eta_G^2\cdot\eta_x^2}{\sigma_y^2}\end{aligned} \tag{4}$$

where σ_y^2 is the output spectrum arithmetic mean (also the output signal energy), η_x^2 is the geometric mean of the input

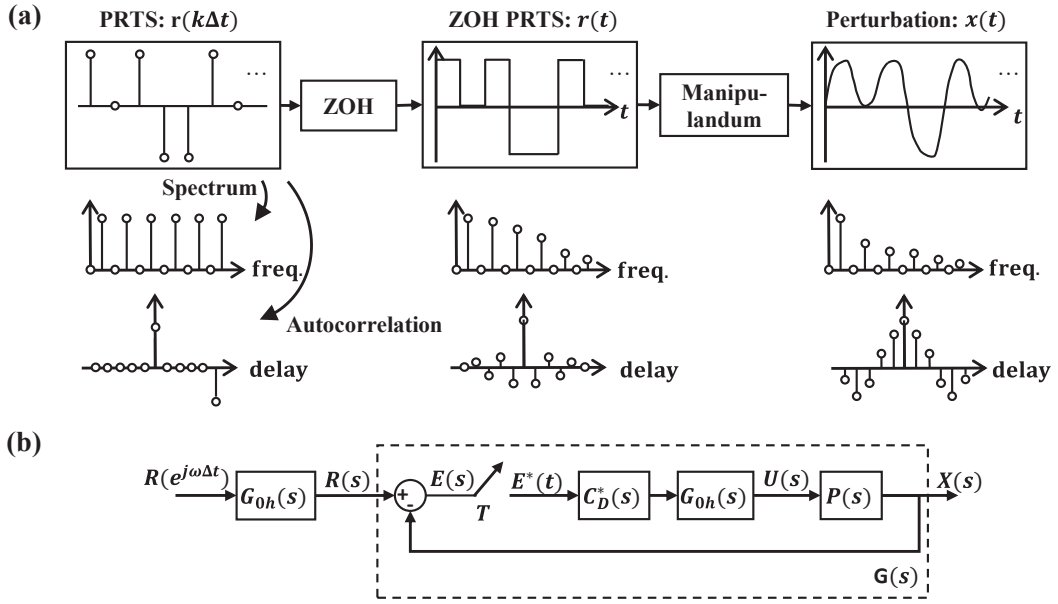

Fig. 1. Physical realization of pseudorandom motion. Changes in signals, spectra, and ACF are shown conceptually. (a) Two-step spectrum modulation. The first source of spectrum modulation is the ZOH that converts a sequence $r(k\Delta t)$ into a continuous-time signal $r(t)$. The second source is the closed-loop manipulandum dynamics which takes $r(t)$ as the reference and generates motion $x(t)$. (b) Block diagram of the system in (a).

spectrum defined in (1), and the geometric mean of the transfer function spectrum η_G^2 is

$$\begin{aligned}\eta_G^2 &= \exp\left[\frac{1}{2\pi}\int_{-\pi}^{\pi}\log|G(e^{j\theta})|^2 d\theta\right] \\ &= \exp\left[f(e^{j\theta})\right]\end{aligned} \tag{5}$$

Substituting $\gamma_x^2\sigma_x^2$ for η_x^2,

$$\gamma_y^2 = \left(\eta_G^2\frac{\sigma_x^2}{\sigma_y^2}\right)\gamma_x^2 = \left(\eta_G^2\frac{R_{xx}(0)}{R_{yy}(0)}\right)\gamma_x^2 \tag{6}$$

and the spectral flatness gain is defined by

$$SFG_{yx} = \frac{\gamma_y^2}{\gamma_x^2} = \eta_G^2\frac{R_{xx}(0)}{R_{yy}(0)}. \tag{7}$$

That is, the output SFM equals to the input SFM multiplied by two factors: the geometric mean of the transfer function spectrum η_G^2, and the ratio of the input signal energy to the output signal energy $R_{xx}(0)/R_{yy}(0)$. In the case where the transfer function $G(z)$ is an all-zero filter of the form $G(z) = 1 + \sum_{k=1}^{M} a_k z^{-k}$, $\eta_G^2 = 1$, and the output SFM becomes the input SFM multiplied by the input-to-output energy ratio [16]. For a general $G(z)$, η_G^2 given in (5) is generally not equal to 1. Manipulating the exponent of η_G^2,

$$\begin{aligned}f(e^{j\theta}) =& \frac{1}{2\pi}\int_{-\pi}^{\pi}\log|G(e^{j\theta})|^2 d\theta \\ =& \frac{1}{2\pi}\int_{-\pi}^{\pi}\log|G(e^{-j\theta})|^2 d\theta \\ =& 2\,\mathrm{Re}\left[\frac{1}{2\pi j}\oint_{\Gamma}\frac{\log G(z^{-1})}{z}dz\right]\end{aligned} \tag{8}$$

where Γ is the unit circle in the z-plane. The function of z inside the integral has a simple pole at $z = 0$. Assume that $G(z^{-1})$ is analytic on and inside the unit circle, by using the Residue theorem, the contour integral shown above can be evaluated as

$$\oint_{\Gamma}\frac{\log G(z^{-1})}{z}dz = 2\pi j\left(\lim_{z\to 0} z\frac{\log G(z^{-1})}{z}\right) \tag{9}$$

Substituting the integral evaluation back in (8) yields

$$f(e^{j\theta}) = 2\,\mathrm{Re}\left[\lim_{z\to 0}\log G(z^{-1})\right]. \tag{10}$$

Now consider a closed-loop system $G(z)$ with all poles and zeros inside the unit circle,

$$G(z) = \frac{b_m z^m + b_{m-1}z^{m-1} + ... + b_0}{z^n + a_{n-1}z^{n-1} + ... + a_0}. \tag{11}$$

Assume that the coefficients a_n and b_m are both nonzero,

$$G(z^{-1}) = z^{-p}\frac{b_m + b_{m-1}z + ... + b_0 z^m}{1 + a_{n-1}z + ... + a_n z^n} \tag{12}$$

where $p = m - n$. Then, $f(e^{j\theta}) = 2\log|b_m|$ and the geometric mean of the transfer function spectrum becomes $\eta_G = \exp[2\log|b_m|] = b_m^2$. Substituting to (7), the input-to-output spectral flatness gain is given by

$$SFG_{yx} = \frac{\gamma_y^2}{\gamma_x^2} = b_m^2\frac{R_{xx}(0)}{R_{yy}(0)} \tag{13}$$

Compared with (7), the first multiplier of the SFG is replaced by b_m^2, the squared leading coefficient of the numerator. It can be interpreted as the extent to which the new output is influenced by the latest input. Note that although $G(z)$ represents the dynamics of a closed-loop manipulandum system in the current context, the derived SFG expression holds for any transfer function satisfying the stability and leading coefficient assumption. In other contexts, $G(z)$ may represent a digital filter or a discrete-time plant model.

B. Band-limited spectral flatness measure

The discrete-time description of a system or signal specifies spectrum information up to the Nyquist frequency. When a high sampling rate is used, the Nyquist frequency could be much greater than the system bandwidth and the maximum frequency of interest. Evaluating the SFM up to the Nyquist frequency may not be appropriate anymore. Instead, evaluating over a limited frequency band would yield representative results. In particular, due to band-limited human motor responses, it is reasonable to analyze the SFM of applied perturbations within a limited frequency band that matches that of the human responses. Given a finite energy time sequence $x(n)$, the band-limited spectral flatness measure (band-limited SFM) is defined as

$$\gamma_x^2(f_{ub}) = \frac{\exp[\frac{1}{2\theta_{ub}} \int_{-\theta_{ub}}^{\theta_{ub}} \log S_{xx}(e^{j\theta}) d\theta]}{\frac{1}{2\theta_{ub}} \int_{-\theta_{ub}}^{\theta_{ub}} S_{xx}(e^{j\theta}) d\theta} \tag{14}$$

with $\theta_{ub} = \left(\frac{f_{ub}}{f_s/2}\right)\pi$ where f_{ub} is the upper bound of the frequency band and f_s is the sampling frequency. Without further specification, the lower bound of the frequency band is 0 Hz. The discrete version of the band-limited SFM is

$$\gamma_x^2(f_{ub}) = \frac{\exp[\frac{1}{N_{ub}} \sum_{n=0}^{N_{ub}-1} \log S_{xx}(n)]}{\frac{1}{N_{ub}} \sum_{n=0}^{N_{ub}-1} S_{xx}(n)} \tag{15}$$

where N_{ub} is the index of the upper-bound frequency. Except for the perfectly flat spectrum, which has a SFM of 1 regardless of the chosen frequency band, the band-limited SFM is a function of frequency band. Figure 2(a) shows the spectrum of a PRTS $r(k\Delta t)$ (top) and the spectrum of the sampled ZOH PRTS $r(nT)$ (bottom) with zero magnitude components removed. The sampling period of the sampled ZOH PRTS is set to $T = 0.02$ s, 10 times smaller than the PRTS update period $\Delta t = 0.2$ s. The spectrum of $r(k\Delta t)$ has a SFM of 1. The band-limited SFM of $r(nT)$ is shown in the top figure in Fig. 2(b). When the spectral flatness is evaluated for a 2.5 Hz frequency band, the band-limited SFM is greater than 0.95. As the frequency band increases, the band-limited SFM drops significantly. The drop is contributed by the inclusion of smaller magnitude spectrum components at higher frequencies.

For a given signal, its band-limited SFM may vary significantly for different frequency bands. Therefore, the value of the band-limited SFM should be interpreted relatively given a frequency band. Comparison of band-limited SFM of different frequency bands should be avoided. Direct comparison with the perfect SFM of 1 is typically not reasonable unless a low frequency band upper bound (about the Nyquist frequency of the $r(k\Delta t)$ in this example) is applied.

By setting a frequency band, high-frequency information is ignored. Whether or not a frequency band is reasonable can be checked by the ratio of signal energy contained in it. Using the sampled ZOH PRTS as an example, the ratio of the signal energy contained in the frequency band to the total energy is plotted in Fig. 2(b) (bottom). A 2.5 Hz frequency band contains over 80% of the total signal energy, and a 5 Hz frequency band contains over 90% of the total signal energy. In industrial systems, system bandwidth is typically 1/5 to 1/20 of the Nyquist frequency [17]. Using a maximum achievable pass band as the frequency band for band-limited SFM evaluation can effectively reduce the impact of unimportant spectrum components.

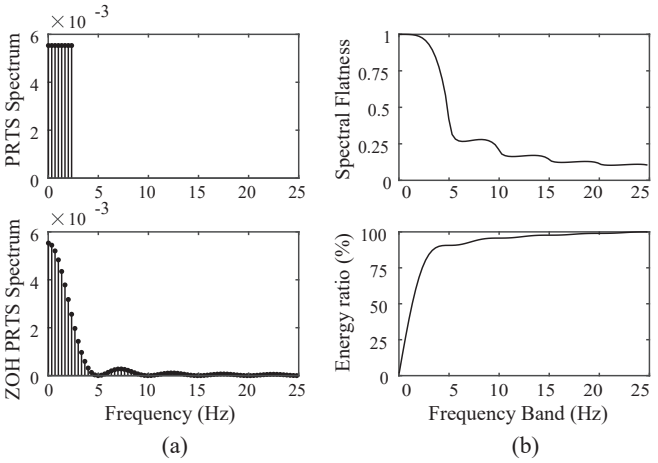

Fig. 2. (a) Spectra of a PRTS (top) and sampled ZOH PRTS (bottom). (b) Band-limited SFM of the sampled ZOH PRTS (top) and the ratio of signal energy contained in the frequency band (bottom).

C. Band-limited spectral flatness gain

Similar to (13), the Band-limited Spectral Flatness Gain (BLSFG) can be defined by

$$SFG_{yx}(f_{ub}) = \frac{\gamma_y^2(f_{ub})}{\gamma_x^2(f_{ub})} \tag{16}$$

where $\gamma_x^2(f_{ub})$ and $\gamma_y^2(f_{ub})$ are defined in (14) and f_{ub} specifies the frequency band upper bound. Both $\gamma_y^2(f_{ub})$ and $\gamma_x^2(f_{ub})$ have a maximum value of 1. When the input signal has a degraded band-limited SFM, that is $\gamma_x^2(f_{ub}) < 1$, $SFG_{yx}(f_{ub})$ can be greater, equal to, or smaller than 1 depending on the value of $\gamma_y^2(f_{ub})$. When $SFG_{yx}(f_{ub}) < 1$, the closed-loop system is a source of flatness degradation. When $SFG_{yx}(f_{ub}) > 1$, the closed-loop system dynamics compensates for the flatness degradation within the frequency band. When $SFG_{yx}(f_{ub}) = 1$, the closed-loop system has a constant gain within the frequency band. Note that the three cases of $SFG_{yx}(f_{ub})$ also apply to SFG_{yx} where the frequency band upper bound is the Nyquist frequency.

IV. Simulation

A. Three cases of BLSFG

Given a SFM-degraded input reference and a closed-loop system dynamics, the BLSFG could be greater, equal to, or smaller than 1 depending on the frequency band. This can be demonstrated by a sampled ZOH PRTS input and a standard second-order system.

In Fig. 3, the spectra of the sampled ZOH PRTS and three system outputs are plotted (top). The output spectra (blue, red, and yellow) are the results of the input spectrum (black) modulated by three second-order systems with specified damping ratio ζ and natural frequency f_n. For each spectrum, the

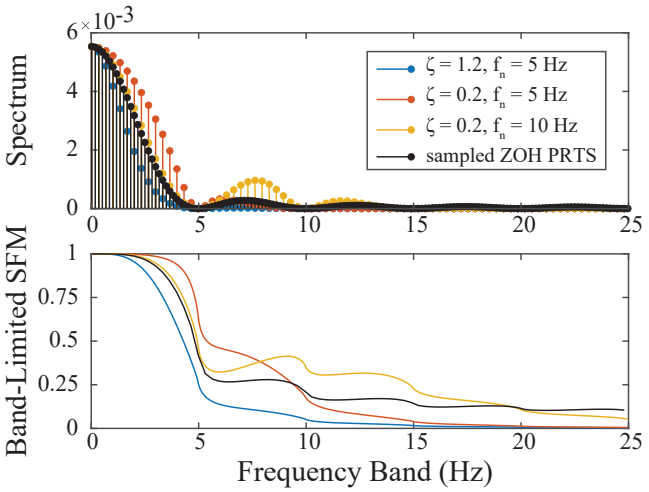

Fig. 3. Spectra of sampled ZOH PRTS and system outputs (top) and their band-limited SFM (bottom). The update period of the PRTS is $\Delta t = 0.20$ s. The sampling period of the discrete-time system is $T = 0.02$ s.

corresponding band-limited SFM are plotted in the bottom figure of Fig. 3. For a specific frequency band, if the output band-limited SFM plot is above the input's, the BLSFG is greater than 1, and vice versa.

The blue plot in Fig. 3 corresponds to the closed-loop system with $\zeta = 1.2$ and $f_n = 5$ Hz. It is an overdamped system in which the output spectrum is always below the input spectrum shown in black. The shape of the output spectrum is observed to be less flat than the input spectrum regardless of the frequency band considered. This observation is confirmed by the band-limited SFM plots where the blue curve is always below the black curve. In this case, the BLSFG does not exceed 1 anywhere. The red plot corresponds to the second closed-loop system with $\zeta = 0.2$ and $f_n = 5$ Hz. It has the same natural frequency as the previous system (blue) but is lightly damped. The output spectrum has greater magnitude between 0 and 5 Hz due to the resonance at 4.8 Hz, leading to a BLSFG greater than 1 in this frequency range. The third system has the same damping ratio as the second system but a higher natural frequency. It has a major spectrum gain between $5 - 10$ Hz. Its band-limited SFM is roughly the same as the input's between $0-5$ Hz, higher between $5-20$ Hz, and lower beyond 20 Hz, corresponding to a BLSFG equal to, greater, and smaller than 1 respectively. If a frequency band up to 8 Hz is considered, the second system (red) is preferred.

B. Case study: generating position perturbation with a linear drive manipulandum

The manipulandum shown in Fig. 4 has been constructed to enable overground human-robot partnered stepping. It also functions as a platform for human motor system identification. The manipulandum can implement a position control as in Fig. 1(b) to provide position perturbations to human subjects. For maximum perturbation quality, the motion control should be designed for maximum achievable spectral flatness.

The manipulandum plant can be model as a mass-damper system, $P(s) = 1/\left(ms^2 + cs\right)$, with mass m and damping

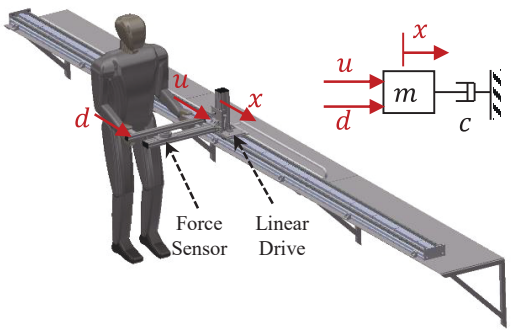

Fig. 4. One degree-of-freedom linear manipulandum: a long-stroke linear drive is mounted on a surface at about waist-height. An extrusion structure with handles extends sideways allows hand interactions.

coefficient c. The system input (position reference), $r(t)$, is provided by a ZOH PRTS with an update period of Δt. The discrete-time controller, operating with a sampling period of T, takes the input reference and generates position perturbation, $x(t)$, as the system output. In the following simulation results, these system parameters are used unless otherwise specified: $m = 10$ kg, $c = 50$ Ns/m, $\Delta t = 0.2$ s, $T = 0.001$ s, and $r(t)$ is obtained by a maximum-length 5^{th} order PRTS with ZOH.

C. Controller design for optimal BLSFG

As observed in Fig. 3, band-limited SFM can be improved by amplifying the system output spectrum over a certain frequency range. A properly designed phase-lead compensator of the form $C(s) = K_p(s + 2\pi f_z)/(s + 2\pi f_p)$ has such capability and is considered here to study the association between the control system properties and the BLSFG. Of the three design parameters, f_z and f_p specify the corner frequencies of 20 dB/dec and -20 dB/dec gain, while K_p scales the overall gain. By choosing positive K_p, f_z and f_p, the closed-loop stability is guaranteed. The discretized controller $C_D(z)$ can be obtained by the bilinear transformation as

$$C_D(z) = K_p \frac{\left(\frac{2/T+2\pi f_z}{2/T+2\pi f_p}\right) z + \left(\frac{-2/T+2\pi f_z}{2/T+2\pi f_p}\right)}{z + \left(\frac{-2/T+2\pi f_p}{2/T+2\pi f_p}\right)}.$$

When $f_z = f_p$, the controller reduces to a proportional controller. The closed-loop system is a second-order system given by

$$\begin{aligned} G(z) = \frac{X(z)}{R(z)} &= \frac{C_D(z)P_0(z)}{1 + C_D(z)P_0(z)} \\ &= \frac{K_p(\beta_1 z + \beta_2)}{z^2 + (K_p\beta_1 - e^{-bT} - 1)z + (K_p\beta_2 + e^{-bT})} \end{aligned} \tag{17}$$

where $b = c/m$, $P_0(z) = \mathcal{Z}[G_{0h}(s)P(s)]$ is the pulse transfer function of the plant and the ZOH and

$$\begin{aligned} \beta_1 &= \frac{m}{c^2}(e^{-bT} - 1) + \frac{T}{c} \\ \beta_2 &= \frac{m}{c^2}(1 - e^{-bT}) - \frac{T}{c}e^{-bT} \end{aligned} \tag{18}$$

are parameters of the ZOH plant model. The controller gain K_p appears in the last two terms of the denominator which

affects both the damping ratio and natural frequency of the position control system. The leading coefficient of the numerator is $K_p\beta_1$, a function of the controller gain and the mass and damping coefficient of the plant. Providing a sampled ZOH PRTS as the input, which has band-limited SFM of $\gamma_r^2(5) = 0.3896$ and $\gamma_r^2(10) = 0.1921$, the BLSFG can be computed using (16). The results of a 5 Hz frequency band ($SFG_{xr}(5)$) and a 10 Hz frequency band ($SFG_{xr}(10)$) are plotted in Figs. 5(a) and 5(b) as a function of the controller gain K_p (top). A BLSFG greater than 1 means that the output band-limited SFM is improved by the closed-loop sytem, and vice versa. It has been shown that the ZOH effect appears on the spectrum as notches at the integer multiples of the sampling frequency and attenuation over the spectrum. To compensate for the flatness degradation due to ZOH, the closed-loop system needs to amplify the frequency components that are attenuated by ZOH. By locating the peaks of $SFG_{xr}(5)$ and $SFG_{xr}(10)$ in Figs. 5(a) and 5(b) and finding their corresponding proportional gain (top), it can be observed that their resonance frequencies are close to f_{ub}, the upper bound of the frequency band (bottom).

When $f_z \neq f_p$, the controller has two additional degrees of freedom to shape the closed-loop spectrum. Selection of f_z and f_p highly depends on the frequency band considered and system capacity. f_p can be set to the desired bandwidth so that spectrum components beyond the desired bandwidth are further attenuated. Typically, the desired bandwidth should be at least 10 times the reference update rate. After fixing f_p, f_z and K_p can then be varied to achieve high BLSFG given a frequency band. Figure 5(c) plots 5 Hz BLSFG of several f_z as a function of K_p. For each curve, the peak (if it exists) occurs when the closed-loop system has a resonance frequency close to 5 Hz. When the BLSFG is evaluated over a 10 Hz frequency band, the results are shown in Fig. 5(d). Similar to the previous result, systems with peak BLSFG have resonance frequencies close to 10 Hz.

D. Disturbance suppression analysis

Human interaction can be modeled as an input disturbance. The designed motion controller not only needs to achieve high spectral flatness but also needs to have sufficient disturbance suppression. Let $r(t)$, $d(t)$, and $x(t)$ respectively denote the input reference, disturbance (due to human interaction), and output, $C(z)$ and $P(z)$ respectively denote the controller and system plant, and a negative feedback control system, $x = (C(r-x)+d)P$. With a lead compensator, the sensitivity of the system output to a disturbance force acting on the plant is $S(z)P(z)$ where $S(z)$ is the sensitivity function. Without assuming knowledge of the disturbance, the peak magnitude of $S(z)P(z)$, or $||SP||_\infty$, indicates the disturbance suppression performance in the worst case. For the systems in Figs. 5(c) and (d) with BLSFG greater than 1, their disturbance suppression characteristics in terms of $||SP||_\infty$ are shown in Figs. 5 (e) and (f).

The control systems that achieve greater than 1 BLSFG have $||SP||_\infty$ of the order of 10^{-4} or lower. This means that the disturbance force due to human interaction can be effectively suppressed while a high BLSFG is achieved.

V. Discussion

Properly designed motion controls can compensate for the SFM degradation of a ZOH PRTS. When a phase-lead compensator is assumed, such controllers lead to a resonance frequency f_r close to $1/\Delta t$ Hz, the update frequency of the original PRTS. The existence of a resonance frequency implies that the closed-loop systems are underdamped. The enhanced BLSFG can be explained by the amplification of the significantly attenuated spectrum components around the resonance frequency. For human system identification, the amplification of higher frequency components enables higher frequency responses of the sensorimotor system to be probed. Controllers of other forms that have properly placed resonance frequency are expected to achieve similar BLSFG enhancement as well. Furthermore, higher order controllers, such as cascaded phase-lead compensators, may be applied to create multiple resonances to increase the maximum achievable BLSFG for a wider frequency band. For a reference signal other than a ZOH PRTS, the optimal controller design may vary; however, the approach of spectrum shape manipulation remains the same.

For controllers with high BLSFG, their disturbance suppression performance has been shown to be satisfactory. The performance was evaluated by the H_∞-norm of the output-to-disturbance sensitivity function, which does not require prior information of force disturbance due to human interaction. In the future, a disturbance observer can be integrated to improve the disturbance suppression performance. The impact of human dynamics on the BLSFG will be studied, and the motion control will be designed with the human interaction dynamics considered.

Besides perturbation quality, safety is an important consideration in human experiments. A flat spectrum perturbation containing high-frequency components may deliver excessive power to human subjects. In addition to the stability analysis of closed-loop systems, energy analysis will be conducted in the future to ensure safety of subjects.

VI. Conclusion

A spectral flatness metric, named the BLSFG, was proposed to quantify the fidelity of the robot motion control and quality of physical perturbations. Closed-loop position control of a manipulandum interacting with a subject at the hand was performed as a case study. The spectral flatness of pseudorandom perturbations was improved with a BLSFG greater than 1 by properly placing the resonance frequency of the closed-loop system. Controller design based on the BLSFG may be applied to a broad class of robotic devices to realize application-specific perturbations in the frequency domain.

Appendix
Derivation of Spectral Flatness Measure

Given a finite energy time sequence $x(n)$, the spectral flatness measure (SFM) is defined as [15]

$$\gamma_x^2 = \frac{\exp\left[\frac{1}{2\pi}\int_{-\pi}^{\pi}\log S_{xx}(e^{j\theta})d\theta\right]}{\frac{1}{2\pi}\int_{-\pi}^{\pi}S_{xx}(e^{j\theta})d\theta} = \frac{\eta_x^2}{\sigma_x^2} \qquad (19)$$

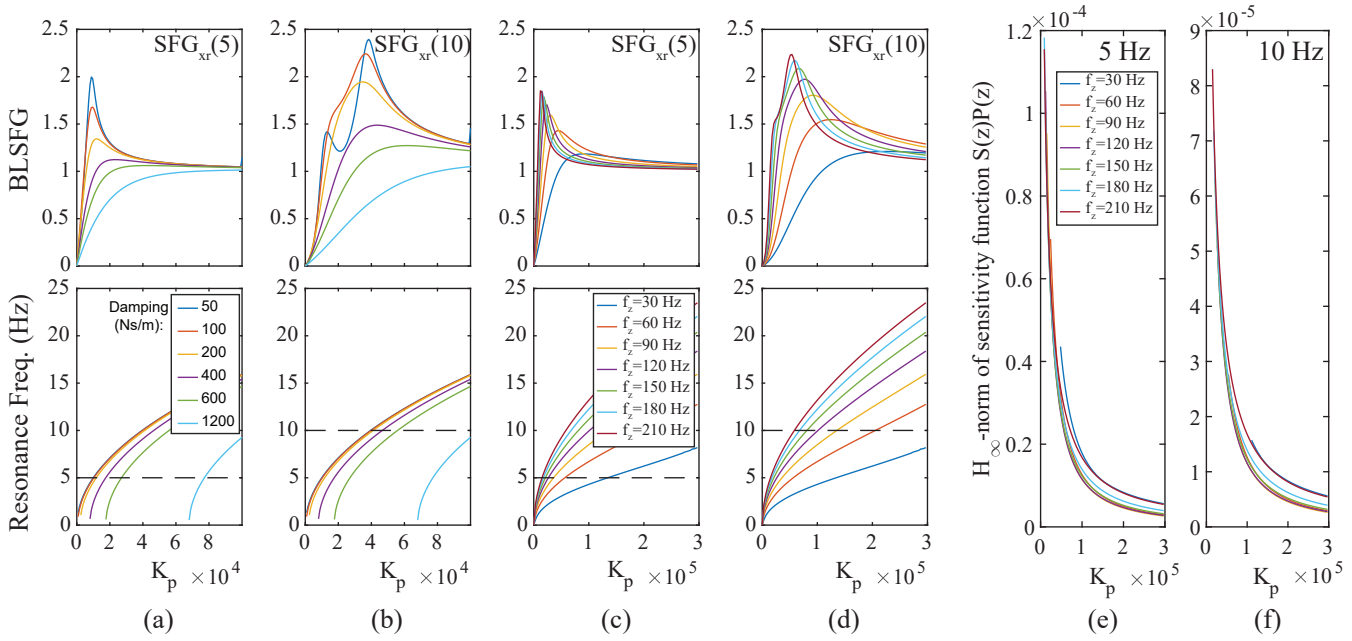

Fig. 5. Phase-lead compensator design based on BLSFG. (a) and (b): 5 Hz and 10 Hz BLSFG (top) and resonance frequency (bottom) of systems with varying proportional gain K_p. (c) and (d): 5 Hz and 10 Hz BLSFG (top) and resonance frequency (bottom) of systems with a phase-lead compensator with a zero at $-2\pi f_z$. (e) and (f): Disturbance suppression characteristics of systems with (e) $SFG_{xr}(5) > 1$ and (f) $SFG_{xr}(10) > 1$. Performance is evaluated by the H_∞-norm of the sensitivity function $S(z)P(z)$.

where $S_{xx}(e^{j\theta})$ is the power spectrum of the time sequence $x(n)$, and η_x^2 and σ_x^2 denote the geometric mean and arithmetic mean of the spectrum. The spectral flatness measure has a maximum value of 1 when the spectrum is perfectly flat. The spectral flatness measure is extensively applied to linear prediction analysis of speech. The derivation of the SFM [16] provides insights into realizing pseudorandom motion in a physical system.

Consider a finite energy time sequence $x(n)$ and let $R_{xx}(\tau)$ denote its autocorrelation and $X(z)$ denote the Z-transform of $x(n)$. The signal energy equals to the autocorrelation with zero delay and can be computed as

$$R_{xx}(0) = \sum_{n=-\infty}^{\infty} x(n)^2 = \frac{1}{2\pi}\int_{-\pi}^{\pi} |X(e^{j\theta})|^2 d\theta. \tag{20}$$

The last equality means that the signal energy is also the mean of the signal power spectrum. The normalized log spectrum is defined as

$$V(\theta) = \log\left(\frac{|X(e^{j\theta})|^2}{R_{xx}(0)}\right) \tag{21}$$

where the power spectrum is normalized by the signal energy (i.e., the spectrum mean) and the logarithm is taken. With normalization shown in (21), a perfectly flat (or constant) spectrum yields a value of zero. For a spectrum that is not perfectly flat, the normalized log spectrum indicates the amount of deviation. One method of measuring the total deviation from the flat spectrum is to take the sum of squared deviation as

$$\frac{1}{2\pi}\int_{-\pi}^{\pi} \frac{1}{2} V^2(\theta) d\theta. \tag{22}$$

This measure penalizes large deviations, but treats positive and negative deviations equally. It is often preferable in practice to assign greater weights to large positive deviations in order to suppress resonance. One of such asymmetric weighted sum that was statistically optimized for speech analysis is given by [18]

$$\mu_X = \frac{1}{2\pi}\int_{-\pi}^{\pi} \exp[V(\theta)] - 1 - V(\theta) d\theta. \tag{23}$$

Substituting (21) into (23), the integral of the first term turns out to be 1 and cancels out the second term, yielding:

$$\begin{aligned} \mu_X &= -\frac{1}{2\pi}\int_{-\pi}^{\pi} V(\theta) d\theta \\ &= -\frac{1}{2\pi}\int_{-\pi}^{\pi} \log\left(\frac{|X(e^{j\theta})|^2}{R_{xx}(0)}\right) d\theta. \end{aligned} \tag{24}$$

The simple sum of squared deviations in (22) has an integrand of quadratic form of $V(\theta)$. Since $V(\theta)$ is already a quadratic expression of the signal magnitude spectrum $|X(e^{j\theta})|$, the integrand in (22) is in fact $4th$ order in terms of the $|X(e^{j\theta})|$. On the other hand, due to the cancellation, the integrand of (24) is quadratic in terms of $|X(e^{j\theta})|$. Equation (24) returns non-positive values, where a value of 0 corresponds to a perfectly flat spectrum. The spectral flatness measure is then defined as

$$\begin{aligned} \gamma_x^2 &= \exp(-\mu_X) \\ &= \exp\left[\frac{1}{2\pi}\int_{-\pi}^{\pi} \log\left(\frac{|X(e^{j\theta})|^2}{R_{xx}(0)}\right) d\theta\right]. \end{aligned} \tag{25}$$

Expanding the fraction inside the log function,

$$\begin{aligned}\gamma_x^2 &= \frac{\exp\left[\frac{1}{2\pi}\int_{-\pi}^{\pi}\log|X(e^{j\theta})|^2 d\theta\right]}{\exp\left[\frac{1}{2\pi}\int_{-\pi}^{\pi}\log R_{xx}(0) d\theta\right]} \\ &= \frac{\exp\left[\frac{1}{2\pi}\int_{-\pi}^{\pi}\log S_{xx}(e^{j\theta}) d\theta\right]}{\frac{1}{2\pi}\int_{-\pi}^{\pi} S_{xx}(e^{j\theta}) d\theta} = \frac{\eta_x^2}{\sigma_x^2}.\end{aligned} \tag{26}$$

This gives the definition of the spectral flatness measure in the same form as (19).

REFERENCES

[1] E. Abele, M. Weigold, and S. Rothenbücher, "Modeling and identification of an industrial robot for machining applications," *CIRP annals*, vol. 56, no. 1, pp. 387–390, 2007.

[2] C. Urrea and J. Pascal, "Design, simulation, comparison and evaluation of parameter identification methods for an industrial robot," *Computers & Electrical Engineering*, vol. 67, pp. 791–806, 2018.

[3] M. Mirbagheri, H. Barbeau, and R. Kearney, "Intrinsic and reflex contributions to human ankle stiffness: variation with activation level and position," *Experimental Brain Research*, vol. 135, no. 4, pp. 423–436, 2000.

[4] L. B. Wood, A. R. Winslow, E. A. Proctor, D. McGuone, D. A. Mordes, M. P. Frosch, B. T. Hyman, D. A. Lauffenburger, and K. M. Haigis, "Identification of neurotoxic cytokines by profiling alzheimer's disease tissues and neuron culture viability screening," *Scientific reports*, vol. 5, p. 16622, 2015.

[5] T. D. Welch and L. H. Ting, "A feedback model explains the differential scaling of human postural responses to perturbation acceleration and velocity," *Journal of Neurophysiology*, vol. 101, no. 6, pp. 3294–3309, 2009.

[6] R. Peterka, "Sensorimotor integration in human postural control," *Journal of neurophysiology*, vol. 88, no. 3, pp. 1097–1118, 2002.

[7] L. Ljung, "System identification," *Wiley encyclopedia of electrical and electronics engineering*, pp. 1–19, 1999.

[8] F. De Groote, J. L. Allen, and L. H. Ting, "Contribution of muscle short-range stiffness to initial changes in joint kinetics and kinematics during perturbations to standing balance: A simulation study," *Journal of biomechanics*, vol. 55, pp. 71–77, 2017.

[9] S. J. Sober, S. Sponberg, I. Nemenman, and L. H. Ting, "Millisecond spike timing codes for motor control," *Trends in neurosciences*, vol. 41, no. 10, pp. 644–648, 2018.

[10] D. C. Lin, C. P. McGowan, K. P. Blum, and L. H. Ting, "Yank: the time derivative of force is an important biomechanical variable in sensorimotor systems," *Journal of Experimental Biology*, vol. 222, no. 18, p. jeb180414, 2019.

[11] D. J. Jilk, S. A. Safavynia, and L. H. Ting, "Contribution of vision to postural behaviors during continuous support-surface translations," *Experimental brain research*, vol. 232, no. 1, pp. 169–180, 2014.

[12] A. Ishida and S. Imai, "Responses of the posture-control system to pseudorandom acceleration disturbances," *Medical and Biological Engineering and Computing*, vol. 18, no. 4, pp. 433–438, 1980.

[13] W. Davies, *System identification for self-adaptive control*. Wiley, 1970.

[14] A. Papoulis and S. U. Pillai, *Probability, random variables, and stochastic processes*. Tata McGraw-Hill Education, 2002.

[15] N. S. Jayant and P. Noll, "Digital coding of waveforms: principles and applications to speech and video," *Englewood Cliffs, NJ*, pp. 115–251, 1984.

[16] A. Gray and J. Markel, "A spectral-flatness measure for studying the autocorrelation method of linear prediction of speech analysis," *IEEE Transactions on Acoustics, Speech, and Signal Processing*, vol. 22, no. 3, pp. 207–217, 1974.

[17] K. J. Åström and B. Wittenmark, *Computer-controlled systems: theory and design*. Courier Corporation, 2013.

[18] F. Itakura, "Speech analysis and synthesis systems based on statistical method," *Doctor of Engineering Dissertation, Dept. of Engineering, Nagoya University, Japan*, vol. 51, pp. 562–574, 1972.